CWE-8
June 7-11, 2026
London, ON, Canada

Rooftop design for urban air mobility (UAM) using CFD simulations

Chao Lin[a], Hideki Kikumoto[b], Yasutomo Takakuwa[c], Ryozo Ooka[d]

[a]*Institute of Industrial Science, The University of Tokyo, Tokyo, Japan, c-lin415@iis.u-tokyo.ac.jp*
[b]*Institute of Industrial Science, The University of Tokyo, Tokyo, Japan, kkmt@iis.u-tokyo.ac.jp*
[c]*Institute of Industrial Science, The University of Tokyo, Tokyo, Japan, takakuwa@iis.u-tokyo.ac.jp*
[d]*Institute of Industrial Science, The University of Tokyo, Tokyo, Japan, ooka@iis.u-tokyo.ac.jp*

SUMMARY

The rooftop wind environment, characterized by flow separation at building edges, poses significant safety challenges for rooftop activities such as roof gardens and urban air mobility (UAM) operations. This study investigates the wind-sheltering performance of rooftop parapets on an isolated building using computational fluid dynamics (CFD) simulations. The simulations systematically vary the parapet height and porosity along the upwind, side, and downwind edges. CFD results for solid parapets are validated against wind tunnel measurements at a 1:200 scale, showing good agreement. Wind conditions are evaluated using volume-averaged statistics within the 0–2 m height range above the rooftop surface, corresponding to the typical occupied zone during rooftop use. A global sensitivity analysis based on the Sobol method identifies the upwind and downwind parapet heights as the dominant parameters affecting wind speed, while the height and porosity of the upwind parapet primarily influence the turbulent and total kinetic energies.

Keywords: *rooftop, wind speed, parapet, fence, UAM, RANS*

1. INTRODUCTION

Urban rooftop environments become increasingly important in the deployment of urban air mobility (UAM) operations. As rooftops are expected to serve as takeoff and landing sites, ensuring safe wind conditions is essential for reliable UAM operation. However, rooftop airflow is highly sensitive to building geometry, particularly the presence of parapets. Previous studies showed that parapets largely alter flow separation, recirculation zones, and turbulence generation (Lin et al., 2026, 2025), yet the combined effects of parapet height and porosity on rooftop wind environments remain insufficiently understood. Moreover, the interactions among multiple parapet parameters create a complex design space that has not been comprehensively quantified. To address these gaps, this study systematically investigates the rooftop wind environment under 729 parapet configurations using computational fluid dynamics (CFD) simulations.

2. SIMULATION SETTINGS

Figure 1 (a) shows the 1:1:2 building model with the building height of H = 40 m. Parapets were installed along all roof edges. Parapets 1, 2 and 3 denote upwind, downwind and side parapets, respectively. Their heights and porosities are denoted as *h1*, *h2*, *h3* and *p1*, *p2*, *p3*. The parapet height was varied from 0 to 4 m at increments of 1 m, and the parapet porosity was set to either solid or 40%. A total of 729 combinations of parapet height and porosity were examined in this study. Figure 1 (b) shows the simulation domain and boundary conditions. The domain comprised 16H, 5.5H, and 9H in the streamwise (x), spanwise (y), and vertical (z) directions, respectively. Owing to the theoretical symmetry of the time-averaged flow field in the y direction, only half of the domain was simulated. Figure 1 (c) shows inflow conditions. The solid line indicates a power-

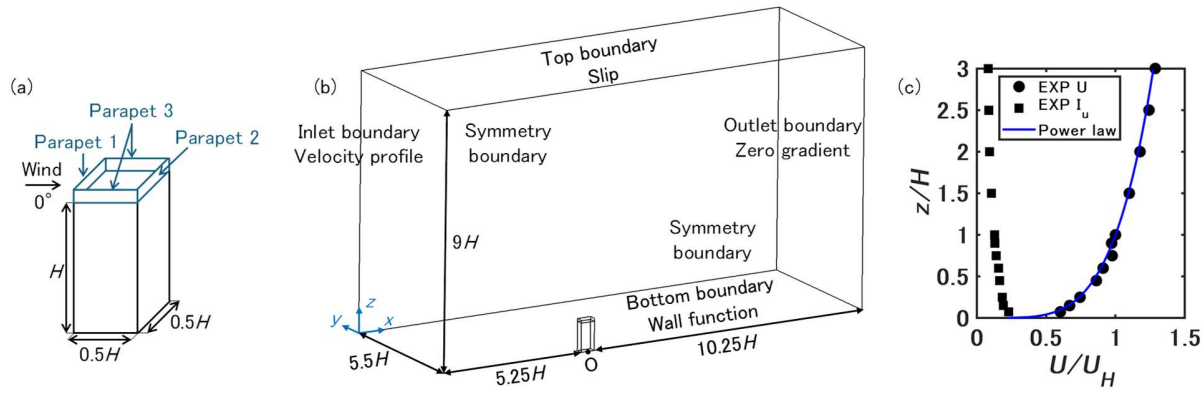

Figure 1: (a) Building and parapet model. (b) Simulation domain. (c) Inflow condition.

law fit with an exponent of 0.22. The wind velocity at 20 m was set as 10 m/s, representing a strong-wind condition that may pose hazards to UAM operation. Flow fields were computed using OpenFOAM v2012, solving the transport equations of the steady-state RANS model with the realizable k–ε turbulence closure. The parapets were modeled as having zero thickness. The aerodynamic effects of porous parapets were represented using a one-dimensional simplification of the porous-media model. The pressure-loss coefficient of the porous parapet was taken as 11.7, following the measurements reported by Tominaga and Shirzadi (2022).

3. RESULTS AND DISCUSSIONS

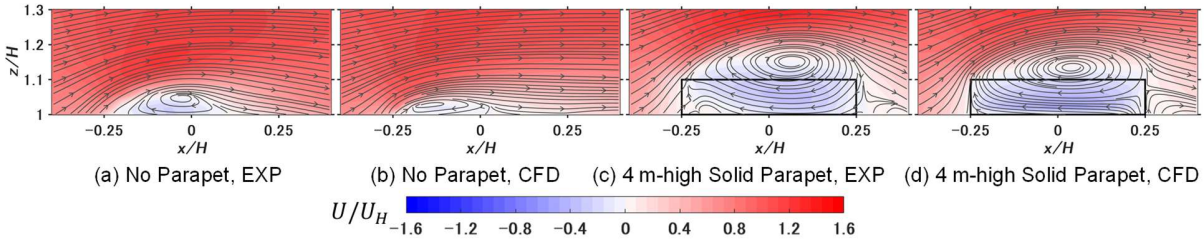

Figure 2: Distributions of time-averaged x-direction wind velocity U in the vertical plane $y/H = 0$ based on wind tunnel experiment and CFD simulations.

The prediction accuracy of the CFD simulations was evaluated against the wind tunnel measurements (Lin et al., 2025). In the experiment, a small recirculation zone is observed in the No-Parapet case, while the presence of parapets clearly enlarges the recirculation region in the experiments (Figure 2(a, b)). The CFD results exhibit generally good agreement with the experiment. Specifically, although the CFD simulation slightly underestimated the recirculation size in the No-Parapet case, it accurately reproduced both the recirculation extent and the vortex center locations for the parapet case (Figure 2(c, d)). Overall, the predictive performance of the CFD simulations is considered satisfactory for the purposes of this study.

The rooftop time-averaged wind speed (WS) and turbulent kinetic energy (TKE) under various parapet configurations are analyzed. Three representative cases are considered as basic cases: Case 1, the configuration without parapets; Case 2, the case with the tallest solid parapet in the study; and Case 3, the case with the tallest porous parapet. Figure 3 shows the WS distributions in the vertical plane $y/H = 0$ for different parapet configurations. Table 1 summarizes the volume-averaged statistics within the 0–2 m height above the rooftop surface, corresponding to the typical

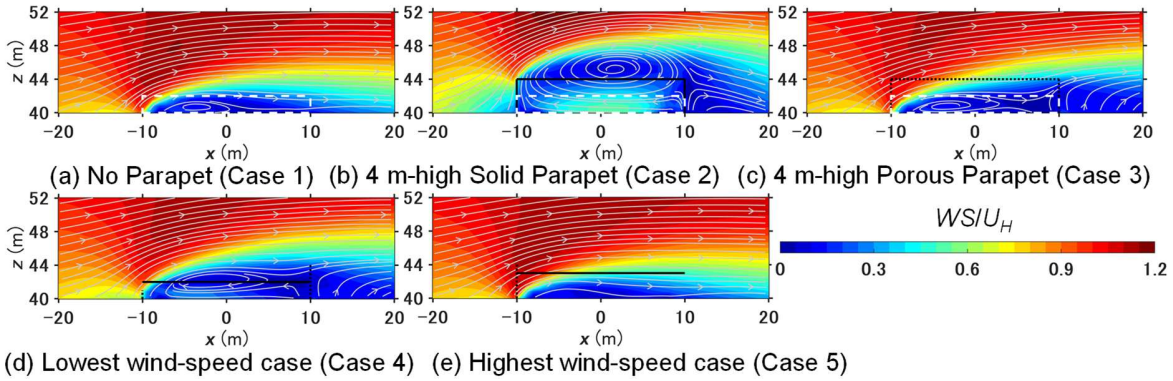

Figure 3: Distributions of time-averaged wind speed in the vertical plane $y/H = 0$. Solid and dot lines refer to solid and porous parapets. The location of lines refers to parapet height. Dash lines refer to the evaluation area.

occupied zone during rooftop use. For basic cases, Case 1 shows a low WS zone near the roof surface because of the separation flow (Figure 3(a)). Although Case 2 (Figure 3(b)) shows a larger size of low WS zone than Case 3 (Figure 3(c)), the WS decrease rate (-15%) is smaller than Case 3 (-32%). The reason is that the solid parapet leaded to strong recirculation flow near the roof surface. The lowest WS case (Case 4) and the highest WS case (Case 5) decreased 50% and increased 12% of volume-averaged WS from Case 1, respectively. Case 4 is characterized as a low porous upwind-parapet, a high porous downwind-parapet and a solid side parapet. Case 5 is characterized as a high porous upwind-parapet, no downwind parapet and a solid side parapet.

Table 1: Volume-averaged statistics within the 0–2 m height range above the rooftop surface with different parapet parameters. Numbers indicate change rate from Case 1. For *p1*, *p2* and *p3*, S means solid parapet, P means porous parapet and N means no parapet. The WS/U_H and k/U_H^2 for Case 1 are 0.35 and 0.08, respectively.

Case	*h1* (m)	*h2* (m)	*h3* (m)	*p1*	*p2*	*p3*	WS/U_H change (%)	k/U_H^2 change (%)	Note
1	0	0	0	N	N	N	-	-	
2	4	4	4	S	S	S	-15	-70	Basic cases
3	4	4	4	P	P	P	-32	-2	
4	1	4	2	P	P	S	-50	-18	Lowest wind-speed case
5	4	0	3	P	N	S	12	-2	Highest wind-speed case
6	4	0	4	S	N	S	-25	-72	Lowest TKE case
7	4	0	1	P	N	P	5	2	Highest TKE case

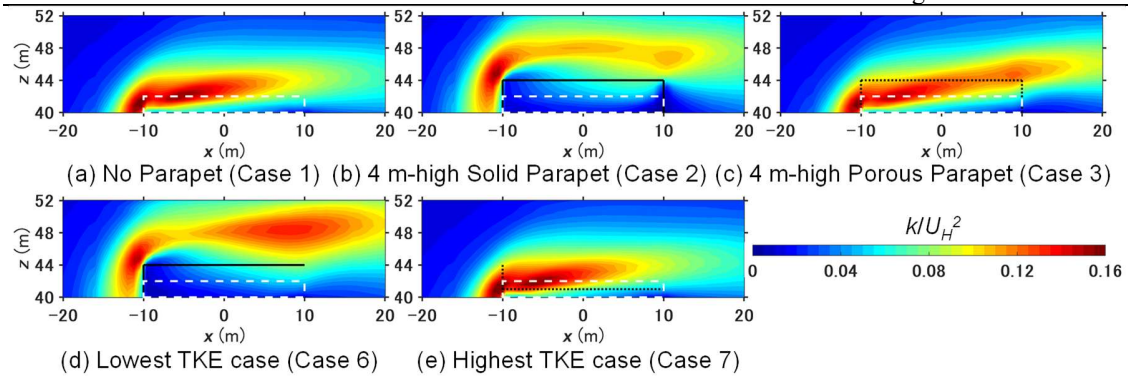

Figure 4: Distributions of turbulent kinetic energy in the vertical plane $y/H = 0$. Line meanings refer to Figure. 3.

Figure 4 shows the TKE distributions in the same vertical plane. For basic cases, Case 1 produces a high-TKE region near the upwind roof edge due to flow separation (Figure 4(a)). Case 2 demonstrates that the solid parapet expands the high-TKE region to the parapet edge (Figure 4(b)).

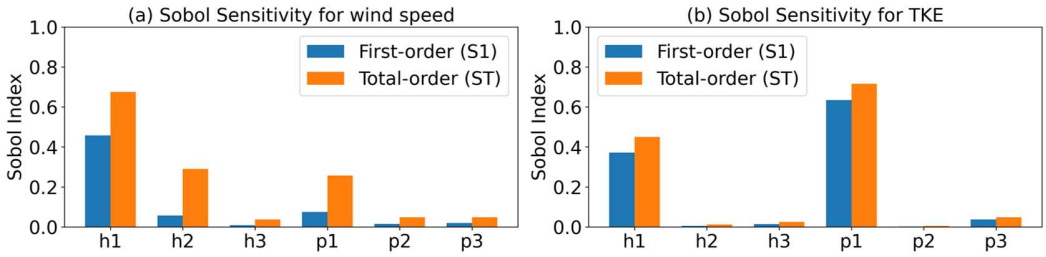

Figure 5: Sobol indices for volume-averaged (a) time-averaged wind speed and (b) turbulent kinetic energy.

In contrast, Case 3 increases TKE near the downwind parapet compared with Case 1 (Figure 4(c)). The lowest-TKE case (Case 6) reduces the volume-averaged TKE by 72% relative to Case 1 by lifting the high-TKE region upward through the use of tall solid parapets along the upwind and side edges. The highest-TKE case (Case 7) slightly increases the volume-averaged TKE by incorporating a tall porous upwind parapet. The global sensitivity analysis of parapet parameters was conducted using the first and total order of Sobol indices (Saltelli et al., 2010), showing that *h1*, *h2* and *p1* are the top influencing factors on the rooftop WS (Figure 5 (a)). Although the detailed results are not shown here, the ten lowest-WS cases share a common feature: a low-porosity upwind parapet combined with a solid side parapet. Conversely, the ten highest-WS cases commonly feature the absence of a downwind parapet. Regarding TKE, *p1* and *h1* are identified as the dominant influencing factors. The ten lowest-TKE cases consistently employ a tall solid upwind parapet together with a solid side parapet, whereas the ten highest-TKE cases typically include a tall porous upwind parapet.

4. CONCLUSIONS

This study systematically examined the influence of parapet height and porosity on rooftop wind conditions through numerical simulation and global sensitivity analysis. The results demonstrate that parapets can substantially modify both wind speed and turbulence intensity above rooftop surfaces. Solid parapets tend to enhance recirculation and reduce wind speed near the surface, whereas porous parapets more effectively moderate separation but may increase turbulence in localized regions. These findings provide practical guidance for optimizing rooftop parapet design to improve aerodynamic conditions for UAM operations.

ACKNOWLEDGEMENTS

This work was supported by the Japan Society for the Promotion of Science (JSPS) KAKENHI Grant Number 24K17398.

REFERENCES

Lin, C., Ooka, R., Takakuwa, Y., Kikumoto, H., 2026. Rooftop wind environment with parapets under upwind building sheltering: A wind tunnel study with implications for urban-air-mobility safety. Build Environ 287, 113854. https://doi.org/10.1016/j.buildenv.2025.113854

Lin, C., Ooka, R., Takakuwa, Y., Kikumoto, H., 2025. Wind tunnel study of Parapet effects on rooftop wind environment with implications for safe urban-air-mobility operations. Build Environ 284, 113509. https://doi.org/10.1016/j.buildenv.2025.113509

Saltelli, A., Annoni, P., Azzini, I., Campolongo, F., Ratto, M., Tarantola, S., 2010. Variance based sensitivity analysis of model output. Design and estimator for the total sensitivity index. Comput Phys Commun 181, 259–270. https://doi.org/10.1016/J.CPC.2009.09.018

Tominaga, Y., Shirzadi, M., 2022. RANS CFD modeling of the flow around a thin windbreak fence with various porosities: Validation using wind tunnel measurements. Journal of Wind Engineering and Industrial Aerodynamics 230, 105176. https://doi.org/10.1016/J.JWEIA.2022.105176